

Fluorine-Free Imidazolium-Based Ionic Liquids with a Phosphorous-Containing Anion as Potential CO₂ Absorbents

Jelliarko Palgunadi, Je Eun Kang, Minserk Cheong, Honggon Kim,[†]
Hyunjoo Lee,^{†,*} and Hoon Sik Kim^{*}

Department of Chemistry and Research Institute of Basic Science, Kyung Hee University, Seoul 130-701, Korea

^{*}E-mail: khs2004@khu.ac.kr

[†]Clean Energy Research Center, Korea Institute of Science and Technology, Seoul 136-791, Korea

^{*}E-mail: hjlee@kist.re.kr

Received May 25, 2009, Accepted June 19, 2009

Solubilities of carbon dioxide (CO₂) in a series of fluorine-free room temperature ionic liquids (RTILs), dialkylimidazolium dialkylphosphates and dialkylimidazolium alkylphosphites, were measured at 313 ~ 333 K and pressures up to 5 MPa. Henry's law coefficients as the solubility parameter of CO₂ in RTILs were derived from the isotherm of fugacity versus CO₂ mole fraction. The CO₂ solubility in a phosphorus-containing RTIL was found to increase with the increasing molar volume of the RTIL. In general, dialkylimidazolium dialkylphosphate exhibited higher absorption capacity than dialkylimidazolium alkylphosphite as long as the RTILs possess an identical cation. Among RTILs tested, 1-butyl-3-methylimidazolium dibutylphosphate [BMIM][Bu₂PO₄] and 1-butyl-3-methylimidazolium butylphosphite [BMIM][BuHPO₃] exhibited similar Henry's law coefficients to 1-butyl-3-methylimidazolium bis(trifluoromethylsulfonyl)imide ([BMIM][Tf₂N]) and 1-butyl-3-methylimidazolium tetrafluoroborate ([BMIM][BF₄]), respectively. The Krichevsky-Kasarnovsky equation was employed to derive the CO₂ solubility parameter (Henry's law coefficient) from the solubility data measured at elevated pressures.

Key Words: CO₂ solubility, Room temperature ionic liquids, Dialkylimidazolium dialkylphosphate, Dialkylimidazolium alkylphosphite

Introduction

Room temperature ionic liquids (RTILs) have been considered as promising alternatives to amine-based absorbents for the separation of CO₂ from natural gas and flue gas because RTILs possess negligible vapor pressure and capability to dissolve CO₂ through physical interaction.^{1,2} The separation of CO₂ through physical interaction is particularly attractive because the stripping of CO₂ from a RTIL can be operated at a much milder condition than that from a conventional aqueous amine-based solution, hence reducing the overall operation cost. Several RTILs have been shown to selectively absorb CO₂ and SO₂ from mixtures of light alkanes, oxygen, hydrogen, nitrogen, or carbon monoxide.³⁻⁵

A number of reports have been published on the CO₂ solubility in RTILs and on the application of RTILs to the reversible CO₂ absorption, but most of them are mainly focused on the use of dialkylimidazolium-based RTILs with costly fluorinated anions such as tetrafluoroborate ([BF₄]),^{1,3,6,7} hexafluorophosphate ([PF₆]),^{1,7,8} and bis(trifluoromethylsulfonyl)imide ([Tf₂N]),^{1,7,9-11} apparently, due to their relatively strong affinities to CO₂.¹² The weak Lewis acid-base interaction of CO₂ with the anion of 1-butyl-3-methylimidazolium tetrafluoroborate ([BMIM][BF₄]) or 1-butyl-3-methylimidazolium hexafluorophosphate ([BMIM][PF₆]) has been demonstrated by an in-situ ATR-IR study.¹³ Besides such specific solute-solvent interaction, the cavity or "free volume" generated within the RTIL molecules for hosting a solute molecule can also be considered as an important factor in determining the solubility of gaseous molecules.^{14,15}

Much effort has been made to develop cost-effective non-fluorinated RTILs with high CO₂ solubility. Modifications on the cations were suggested such as the introduction of a long chain alkyl or an ether linkage to create greater free volume and the incorporation of a CO₂-philic carbonyl functional group.^{16,17} RTILs with a basic anion character like acetate or amino acid residue were also employed as efficient CO₂ absorbents.^{18,19} Even though the aforementioned RTILs exhibited moderate capability of solubilizing CO₂, the application of these RTILs has been restricted, possibly due to their instability toward the hydrolysis²⁰ and also to the costly and complicated preparation steps.^{21,22} In this context, dialkylimidazolium alkylphosphites and dialkylimidazolium dialkylphosphates with a basic anion deserve to receive a great attention because of their easy and cost-effective preparation and high stability toward hydrolysis.²³

Herein, we wish to report in detail on the capability of a series of dialkylimidazolium alkylphosphites and dialkylimidazolium dialkylphosphates to capture CO₂. The Krichevsky-Kasarnovsky equation was employed to derive the CO₂ solubility parameter (Henry's law coefficient) from the solubility data measured at elevated pressures.^{24,25}

Experimental

General procedure. All of the chemicals (purities 98 ~ 99%) used for the synthesis of RTILs were purchased from Aldrich Chemicals Co. and used as received. 1-Butyl-3-methylimidazolium tetrafluoroborate ([BMIM][BF₄]) and 1-butyl-3-methylimidazolium bis(trifluoromethylsulfonyl)imide ([BMIM]

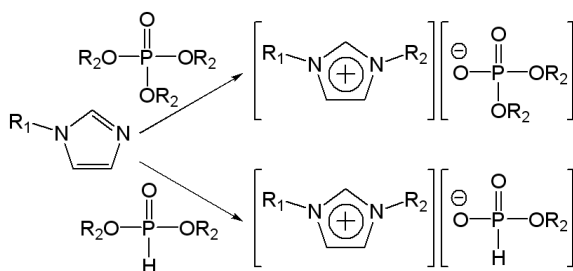
[Tf₂N]) were purchased from Aldrich Chemicals Co. CO₂ gas with purity of 99.9% was purchased from Sin Yang Gas, Korea.

¹H NMR spectra were recorded on a 400 MHz Bruker NMR spectrometer. Densities of neat RTILs were carefully measured at 313.15, 323.15, and 333.15 K at an ambient pressure. In a typical density experiment, a RTIL was loaded in a 5.573 ± 0.004 mL pycnometer (previously calibrated using distilled water at 298.15 K) immersed in an ethylene glycol bath. The weight of RTIL was measured using a Mettler AJ180 balance with an accuracy of 10⁻⁴ g. Water contents in RTILs were determined using a Karl-Fischer Moisture Titrator (MKC-520, KEM Co. Ltd.).

Synthesis of RTILs. All the RTILs under investigation were obtained from the alkylation of 1-alkylimidazole with trialkylphosphate or dialkylphosphite at 90 ~ 120 °C in the absence of solvent as shown in Scheme 1, according to the literature procedures.^{23,26}

The prepared RTILs, 1,3-dimethylimidazolium dimethylphosphate ([DMIM][Me₂PO₄]), 1-ethyl-3-methylimidazolium diethylphosphate ([EMIM][Et₂PO₄]), and 1-butyl-3-methylimidazolium dibutylphosphate ([BMIM][Bu₂PO₄]), 1,3-dimethylimidazolium methylphosphite ([DMIM][MeHPO₃]), 1-ethyl-3-methylimidazolium ethylphosphite ([EMIM][EtHPO₃]), 1-butyl-3-methylimidazolium butylphosphite ([BMIM][BuHPO₃]), and 1-butyl-3-methylimidazolium methylphosphite ([BMIM][MeHPO₃]) were dried under vacuum (<1 mbar) at 348 K at least for 8 h before use to completely eliminate the residual volatiles and moisture.

CO₂ solubility measurement. CO₂ solubility measurements were carried out based on the isochoric saturation method.^{3,10,27} A stainless steel-made solubility test apparatus consisting of an equilibrium cell (EC) and a gas reservoir (GR) was constructed in an oven as illustrated in Fig. 1. The apparatus was equipped with dual pressure transducers, P1 for measuring pressures close to atmospheric pressure (OMEGA Engineering PX309-030AI, 0 to 207 kPa, accuracy 0.25% full scale) and the other one (P2) for high pressure reading up to 7 MPa (OMEGA Engineering PX32B1-1KGV, accuracy 0.25% full scale). The CO₂ solubility measurement was conducted at low pressures first and then at high pressures. Volume of the EC was measured by filling it with distilled water at room temperature. Volumes of the GR and the rest of the system were determined from nitrogen gas expansion employing *pVT* relation. The solubility test unit was placed in an isothermal oven



Scheme 1. Synthesis of dialkylimidazolium dialkylphosphate and dialkylimidazolium alkylphosphite ($R_1 = \text{CH}_3$, and $n\text{-C}_4\text{H}_9$; $R_2 = \text{CH}_3$, C_2H_5 , and $n\text{-C}_4\text{H}_9$).

and the inside temperature was carefully controlled with an accuracy of ± 0.1 K.

In a typical experiment, a known quantity of a RTIL was loaded into the EC and degassed under vacuum at 343 K at least for 2 h prior to each test. At a specified oven temperature, the valve (V4) connecting EC and GR was closed to separate these vessels. CO₂ was fed from the CO₂ supply cylinder to the GR through V2 and V3, and the amount of gas at equilibrium was calculated from the *pVT* relation. CO₂ was then brought into contact with the absorbent in the EC by opening V4 and the absorbent was then stirred vigorously to facilitate the CO₂ absorption. After the absorption reached equilibrium, the amount of dissolved gas was calculated from a difference between the initial gas concentration in the GR and the concentration in the gaseous phase.

The moles of dissolved CO₂ in a RTIL (n_2^{liq}) can be obtained from Eq. (1) on the assumption that the gaseous phase consists of only pure CO₂ due to the negligible vapor pressure of RTIL,

$$n_2^{\text{liq}} = \frac{p_{\text{ini}} V_{\text{GR}}}{[Z_2(p_{\text{ini}}, T_{\text{ini}})RT_{\text{ini}}]} - \frac{p_{\text{eq}}(V_{\text{tot}} - V_{\text{liq}})}{[Z_2(p_{\text{eq}}, T_{\text{eq}})RT_{\text{eq}}]} \quad (1)$$

where p_{ini} and T_{ini} are the initial pressure and temperature in the first *pVT* determination (in the GR), and p_{eq} and T_{eq} are the pressure and the temperature at equilibrium, respectively. V_{tot} is the total volume of the entire solubility apparatus, V_{liq} is volume of the absorbent which is assumed to be constant over the entire range of pressure, and Z_2 is the compressibility factor for the pure component 2, the solute (CO₂).

At pressures close to atmosphere, Z_2 was calculated using Eq. (2) employing the second virial coefficients taken from the compilation by Dymond and Smith.²⁸

$$Z_2 = 1 + \frac{pB_{22}}{RT} \quad (2)$$

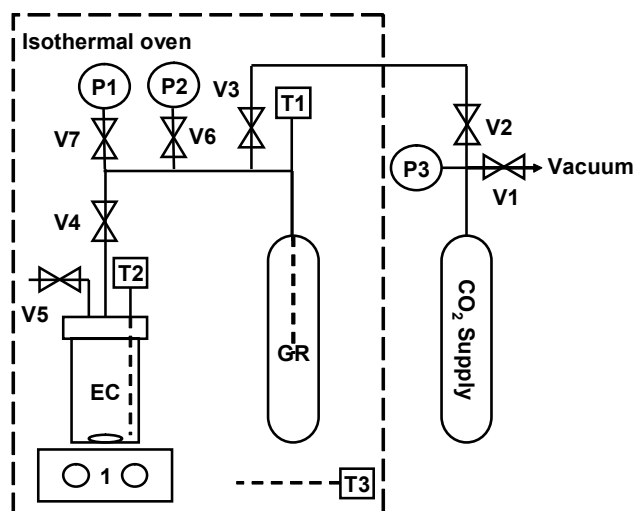


Figure 1. Schematic diagram of the apparatus for CO₂ solubility test: (EC), equilibrium cell; (GR), gas reservoir; (V1-7), valves; (T1-3), K-type thermocouples; (P1-3), pressure transducers; (1), magnetic stirrer.

The solubility of CO₂ expressed in a mole fraction (x_2) and in a volume basis (c) was calculated according to Eq. (3) and Eq. (4), respectively.

$$x_2 = \frac{n_2^{\text{liq}}}{n_1^{\text{liq}} + n_2^{\text{liq}}} \quad (3)$$

$$c = \frac{n_2^{\text{liq}}}{V_{\text{RTIL}}} \text{ mol} \cdot \text{L}^{-1} \quad (4)$$

At a very low solute concentration in an absorbent, the solubility can be expressed in terms of Henry's law coefficient as Eq. (5)

$$H_{2,1}(p, T) \equiv \lim_{x_2 \rightarrow 0} \frac{f_2(p, T, x_2)}{x_2} \quad (5)$$

where $f_2(p, T, x_2)$ is the fugacity of component 2 (CO₂).

At an equilibrium state, the fugacities of a component in the liquid phase and in the vapor phase are equal and are expressed as

$$f_2^{\text{liq}}(p, T, x_2) = f_2^{\text{vap}}(p, T, y_2) = \phi_2(p, T, y_2)y_2p \quad (6)$$

where $\phi_2(p, T, y_2)$ is the fugacity coefficient of component 2, y_2 is the mole fraction of component 2 in the gaseous phase, and p is the total pressure. Since RTILs have negligible vapor pressures, y_2 becomes unity. Thus, Eq. (6) can turn to

$$f_2^{\text{liq}}(p, T, x_2) = \phi_2(p, T, y_2)y_2p = \phi_2(p, T)p \quad (7)$$

where

$$\phi_2(p, T) = \exp \left[\frac{pB_{22}(T)}{RT} \right] \quad (8)$$

At a very low solute concentration in an absorbent, Eq. (5) can be rewritten as

$$H_{2,1}(p, T) = \lim_{x_2 \rightarrow 0} \frac{f_2(p, T, x_2)}{x_2} = \lim_{x_2 \rightarrow 0} \frac{\phi_2(p, T)p}{x_2} \quad (9)$$

In the limit as $x_2 \rightarrow 0$, Henry's law coefficient is simply calculated using Eq. (10).

$$H_{2,1}(p, T) \approx \frac{\phi_2(p, T)p}{x_2} \quad (10)$$

Based on the solubility data, Henry's law coefficient was obtained from the slope of an isotherm linear fit of fugacity versus mole fraction. The pressure of CO₂ at elevated pressures were correlated with the fugacity over the mole fraction of dissolved CO₂ employing the Krichevsky-Kasarnovsky equation (11)

$$\ln \frac{f_2^{\text{vap}}}{x_2} = \ln H_{2,1}^{\text{KK}} + \frac{V_2^{\infty,1}(p - p_1^{\text{S}})}{RT} \quad (11)$$

where p_1^{S} is the saturated vapor pressure of component 1 (RTIL), $H_{2,1}^{\text{KK}}$ is Henry's law coefficient of the solute calculated using the Krichevsky-Kasarnovsky equation at the pressure of p_1^{S} , and $V_2^{\infty,1}$ is the volume of solute (CO₂) in the RTIL at infinite dilution, which is assumed to be constant over the entire range of pressure. The variable p_1^{S} can be considered as zero due to a negligible vapor pressure of RTIL and f_2^{vap} can be substituted by the fugacity of pure CO₂. As a result, Eq. (11) can be reduced to Eq. (12).

$$\ln \frac{f_2^{\text{vap}}}{x_2} = \ln H_{2,1}^{\text{KK}} + \frac{V_2^{\infty,1}}{RT} p \quad (12)$$

where the fugacity $f_2(p, T)$ can be replaced by $\phi_2(p, T)p$.

At elevated pressure conditions, the fugacity coefficient (ϕ_2) of CO₂ was calculated using an EOS program based on the equation of state given by Span and Wagner.²⁹

A linear fit of the natural logarithm of the ratio of fugacity to the solubility of CO₂ ($\ln \frac{f_2^{\text{vap}}}{x_2}$) versus the CO₂ pressure (p) at equilibrium was constructed from the Krichevsky-Kasarnovsky equation from which two solubility parameters, Henry's law coefficient ($H_{2,1}^{\text{KK}}$) and the CO₂ partial molar volume ($V_2^{\infty,1}$) in RTIL at various temperatures can be obtained. In the present paper, only Henry's law coefficients are reported.

Results and Discussion

Physical properties of RTILs. The experimental densities (ρ) and the molar volumes (V_m) of neat dialkylimidazolium dialkylphosphates and dialkylimidazolium alkylphosphites, measured at 313.15, 323.15, and at 333.15 K and at atmospheric pressure, were listed in Table 1. In general, the densities of the RTILs were little influenced by the variation of temperature. However, differently from common organic compounds, the density of a homologous series of RTILs significantly decreased with increasing chain length of the alkyl groups on the cation and/or the anion. Such a density behavior in a homolog series of asymmetric imidazolium-based ionic liquids is also well documented in many literatures.^{7,11,23,30,31}

As expected, in a homologous series of RTILs, the molar volume increased with the increase of the chain length of the alkyl group or groups on the cation and/or the anion, as going from [DMIM][Me₂PO₄] to [BMIM][Bu₂PO₄] and from [DMIM][MeHPO₃] to [BMIM][BuHPO₃]. The correlation of the molar volume with the alkyl chain length is well described in the literatures.^{11,15,16} It is also observed that the molar volume of dialkylimidazolium dialkylphosphate is always larger than that of dialkylimidazolium alkylphosphite, implying that the size of the dialkylphosphate anion is larger than that of alkylphosphite anion.

CO₂ solubility measurements. CO₂ solubility measurement was performed at pressures close to atmosphere and at temperatures of 313.15, 323.15, and 333.15 K. The amount of dissolved CO₂ was calculated based on a pressure-decay obser-

Table 1. Experimental densities (ρ) and molar volumes (V_m) of neat RTILs at different temperatures

$T = 313.15 \text{ K}$		$T = 323.15 \text{ K}$		$T = 333.15 \text{ K}$	
$\rho/\text{g}\cdot\text{cm}^{-3}$	$V_m/\text{mL}\cdot\text{mol}^{-1}$	$\rho/\text{g}\cdot\text{cm}^{-3}$	$V_m/\text{mL}\cdot\text{mol}^{-1}$	$\rho/\text{g}\cdot\text{cm}^{-3}$	$V_m/\text{mL}\cdot\text{mol}^{-1}$
[DMIM][Me ₂ PO ₄]					
1.2510	177.6	1.2444	178.5	1.2380	179.5
[EMIM][Et ₂ PO ₄]					
1.1386	233.4	1.1321	233.4	1.1255	234.8
[BMIM][Bu ₂ PO ₄]					
1.0400	335.0	1.0337	337.1	1.0271	339.2
[DMIM][MeHPO ₃]					
1.2332	155.8	1.2281	156.5	1.2222	157.2
[EMIM][EtHPO ₃]					
1.1492	191.6	1.1428	192.7	1.1363	193.8
[BMIM][BuHPO ₃]					
1.0661	259.2	1.0597	260.7	1.0535	262.3
[BMIM][MeHPO ₃]					
1.1352	206.3	1.1288	207.5	1.1226	208.7

Table 2. List of variation of Henry's law coefficient with temperature

T/K	$H_{2,1}/\text{MPa}^a$	$H_{2,1}^{\text{KK}}/\text{MPa}^b$	Error ^c	RD ^d
[DMIM][Me ₂ PO ₄] + CO ₂				
313.15	10.64	10.66	0.12	0.19
323.15	12.72	13.03	0.03	2.36
333.15	15.22	15.77	0.15	3.52
[EMIM][Et ₂ PO ₄] + CO ₂				
313.15	6.99	6.94	0.03	0.73
323.15	8.12	8.14	0.04	0.24
333.15	9.66	9.42	0.02	2.55
[BMIM][Bu ₂ PO ₄] + CO ₂				
313.15	4.98	5.19	0.02	3.94
323.15	5.76	5.70	0.02	1.14
333.15	6.85	6.47	0.03	5.93
[DMIM][MeHPO ₃] + CO ₂				
313.15	11.48	11.80	0.08	2.69
323.15	13.60	13.89	0.12	2.07
333.15	16.35	16.91	0.20	3.33
[EMIM][EtHPO ₃] + CO ₂				
313.15	9.18	9.65	0.04	4.82
323.15	10.73	10.55	0.02	1.66
333.15	12.36	12.03	0.03	2.74
[BMIM][BuHPO ₃] + CO ₂				
313.15	6.30	6.38	0.03	1.23
323.15	7.51	7.28	0.04	3.04
333.15	8.52	8.09	0.04	5.32
[BMIM][MeHPO ₃] + CO ₂				
313.15	8.68		0.08	
323.15	9.97		0.05	
333.15	11.29		0.12	

^aBased on measurements at close to atmospheric pressure. ^bObtained from the Krichevsky-Kasarnovsky equation. ^cStandard errors of the isotherm slopes measured at close to atmospheric pressure. ^d|RD| = $|(H_{2,1}^{\text{KK}} - H_{2,1})/H_{2,1}| \times 100$.

variation. The CO₂ solubility on a mole fraction (x_2) and a volume basis (c) and the CO₂ equilibrium pressure (p) above the liquid absorbent are listed in Table S-1 (Supplementary Information). The solubility of CO₂ increased with the pressure rise for all of

the RTILs tested. Moreover, the mole fraction increased linearly with the pressure up to 0.17 MPa, inferring the validity of Henry's law within the given pressure range. Table 2 lists Henry's law coefficients (on the mole fraction scale) at various temperatures including the standard error of the isotherm slopes from the solubility measurements at pressure close to atmosphere. The absolute values of relative deviations (|RD|) of Henry's law coefficients resulted from the Krichevsky-Kasarnovsky equation and from measurements at pressure close to atmosphere are also given in the same table. The relative deviations less than 5.0% were obtained except for [BMIM][BuHPO₃] and [BMIM][Bu₂PO₄].

Based on the raw data of CO₂ solubility measurements close to atmospheric pressure, an empirical equation (13) proposed by Krause and Benson³² was employed to show the dependence of Henry's law coefficient on temperature.

$$\ln[H_{2,1}(T)/10^5 \text{ Pa}] = \sum_{i=0}^n B_i(T/\text{K})^{-i} \quad (13)$$

The optimized coefficients B_i ($i = 0 \sim 2$) using a linear regression calculation of multiple variables are listed in Table S-2 (Supplementary Information) as well as the average absolute deviation (AAD) of each compound, which is considered as the precision of the experimental data.

It was reported that the solubility of CO₂ in a dialkylimidazolium-based ionic liquid bearing a fluorinated anion increases with the increasing carbon number of the alkyl group on the cation.^{10,33,34} Such a solubility improvement was attributed to the increase of the void volume created in an ionic liquid caused by the presence of larger sized alkyl group on a dialkylimidazolium.^{15,35} A similar phenomenon was also observed for the dissolution of CO₂ in dialkylimidazolium dialkylphosphates or in dialkylimidazolium alkylphosphites. The size effect of the alkyl group on the cation can be clearly seen from the comparison of the CO₂ solubility in [DMIM][MeHPO₃] with that in [BMIM][MeHPO₃]. The CO₂ solubility in the former is much lower than that in the later. The size of the anion also exerted the similar effect, exhibiting higher CO₂ solubility in [BMIM][BuHPO₃] than in [BMIM][MeHPO₃].

As shown in Fig. 2, the CO₂ solubility measured at 0.1 MPa in dialkylimidazolium dialkylphosphates and in dialkylimidazolium alkylphosphites increases significantly with increasing chain length of the alkyl group. The solubility of CO₂ in these RTILs were found in the order of [DMIM][MeHPO₃] \approx [DMIM][Me₂PO₄] < [EMIM][EtHPO₃] \leq [BMIM][MeHPO₃] < [EMIM][Et₂PO₄] < [BMIM][BuHPO₃] < [BMIM][Bu₂PO₄], which is in good agreement with the order of molar volume. These results support the previous finding that there is a close correlation between the molar volume of RTIL under investigation and the CO₂ solubility, as was similarly observed in the other RTILs-CO₂ systems.^{10,11,33-35}

Fig. 3 displays the effect of temperature on the solubility of CO₂. The natural logarithm of Henry's law coefficients, calculated using the Krichevsky-Kasarnovsky equation and plotted, are relatively well matched with the smoothed data correlation from Eq. (13). The negative slopes of the correlations for all the RTILs imply that the CO₂ solubility reduces as the ab-

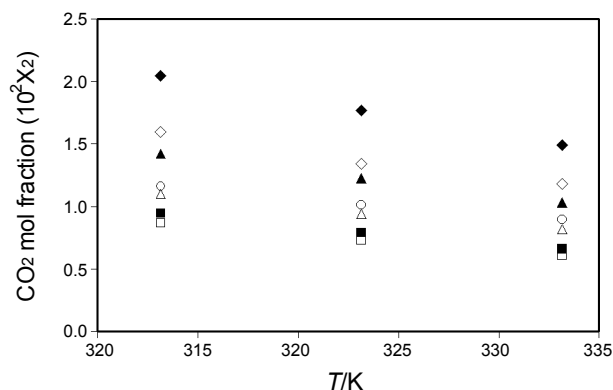


Figure 2. Correlation of CO₂ solubility and temperature at 0.1 MPa of CO₂: (■), [DMIM][Me₂PO₄]; (▲), [EMIM][Et₂PO₄]; (◆), [BMIM][Bu₂PO₄]; (□), [DMIM][MeHPO₃]; (△), [EMIM][EtHPO₃]; (◇), [BMIM][BuHPO₃]; (○), [BMIM][MeHPO₃].

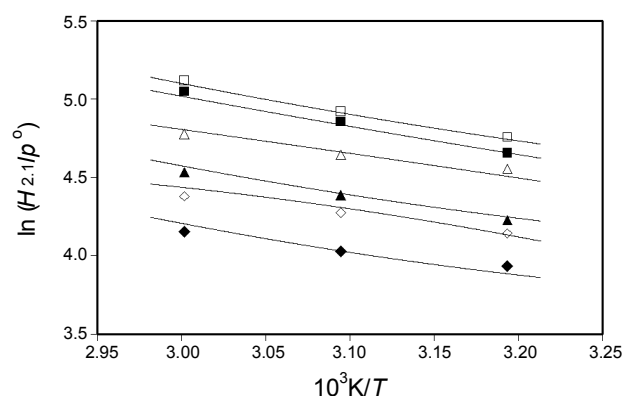


Figure 3. Variation of Henry's law coefficient (calculated from elevated pressure data using the Krichevsky-Kasarnovsky equation) at different temperature of absorption ($p^{\circ} = 101325$ Pa): (■), [DMIM][Me₂PO₄]; (▲), [EMIM][Et₂PO₄]; (◆), [BMIM][Bu₂PO₄]; (□), [DMIM][MeHPO₃]; (△), [EMIM][EtHPO₃]; (◇), [BMIM][BuHPO₃]. Lines represent the smoothed data correlation using Eq. (13) and the parameters in Table S-2.

sorption temperature rises.

For comparison, the CO₂ solubilities in [BMIM][BF₄] and [BMIM][Tf₂N], most frequently studied fluorinated RTILs for CO₂ absorption, were also measured at 313.15 K. As can be seen in Table 3, CO₂ solubilities in [BMIM][Bu₂PO₄] and [BMIM][BuHPO₃] are higher than that in [BMIM][BF₄] as indicated by Henry's law coefficients. More surprisingly, the solubility of CO₂ in [BMIM][Bu₂PO₄] is comparable to that in [BMIM][Tf₂N], suggesting that [BMIM][Bu₂PO₄] could be used as an alternative to the costly RTILs with a fluorinated anion.

Conclusion

The ability of a series of dialkylimidazolium dialkylphosphates and dialkylimidazolium alkylphosphites to capture CO₂ was investigated at various temperatures and pressures and Henry's law coefficients for these RTILs were newly presented. The CO₂ solubility in dialkylimidazolium dialkylphosphates and dialkylimidazolium alkylphosphites is strongly influenced

Table 3. Comparison of Henry's law coefficients for CO₂ in several RTILs

Compound	<i>T</i> /K	<i>H</i> _{2,1} /MPa	Ref.
[BMIM][Bu ₂ PO ₄]	313.15	4.98	This work
[BMIM][BuHPO ₃]	313.15	6.30	This work
[BMIM][BF ₄]	313.15	7.63	This work ^a
[BMIM][BF ₄]	313.99	7.51	[3]
[BMIM][Tf ₂ N]	313.15	4.01	This work ^a
[BMIM][Tf ₂ N]	313.24	4.33	[10]

^aSolubility data is given in the Supplementary Information.

by the chain length of alkyl group in the dialkylimidazolium cation as well as in the dialkylphosphate or alkylphosphite anion: the longer the alkyl chain the larger the CO₂ solubility. Higher solubility of CO₂ in dialkylimidazolium dialkylphosphates than in dialkylimidazolium alkylphosphites seems to be a consequence of the presence of one more alkyl group in the anion, which might contribute to create larger free volume to accommodate more CO₂ molecules. In terms of mole fraction, the CO₂ solubility in [BMIM][Bu₂PO₄] was comparable to that in [BMIM][Tf₂N], which is known as one of the most effective RTILs for CO₂ capture so far reported.

In summary, phosphorous-containing RTILs, dialkylimidazolium dialkylphosphates and dialkylimidazolium alkylphosphites showed relatively high capability to dissolve CO₂. The CO₂ solubility seems to be largely determined by the molecular structure of the RTIL employed, although specific intermolecular interactions between RTIL and CO₂ cannot be ruled out.

Acknowledgments. This work was supported by the Korea Science and Engineering Foundation (KOSEF) grant funded from the Ministry of Education, Science and Technology (MEST) of Korea for the Center for Next Generation Dye-sensitized Solar Cells (No. 2009-0063367).

References

- Baltus, R. E.; Counce, R. M.; Culbertson, B. H.; Luo, H.; DePaoli, D. W.; Dai, S.; Duckworth, D. C. *Sep. Sci. Technol.* **2005**, *40*, 525.
- Zhang, J.; Zhang, S.; Dong, K.; Zhang, Y.; Shen, Y.; Lv, X. *Chem. Eur. J.* **2006**, *12*, 4021.
- Jacquemin, J.; Costa Gomes, M. F.; Husson, P.; Majer, V. *J. Chem. Thermodyn.* **2006**, *38*, 490.
- Anderson, J. L.; Dixon, J. K.; Brennecke, J. F. *Acc. Chem. Res.* **2007**, *40*, 1208.
- Pennline, H. W.; Luebke, D. R.; Jones, K. L.; Myers, C. R.; Morsi, B. I.; Heintz, Y. J.; Ilconich, J. B. *Fuel Proc. Technol.* **2008**, *89*, 897.
- Costantini, M.; Toussaint, V. A.; Shariati, A.; Peters, C. J.; Kikic, I. *J. Chem. Eng. Data* **2005**, *50*, 52.
- Kim, Y. S.; Choi, W. Y.; Jang, J. H.; Yoo, K. P.; Lee, C. S. *Fluid Phase Equilib.* **2005**, *228-229*, 439.
- Pérez Salado Kamps, A.; Tuma, D.; Xia, J.; Maurer, G. *J. Chem. Eng. Data* **2003**, *48*, 746.
- Kumelan, J.; Pérez Salado Kamps, A.; Tuma, D.; Maurer, G. *J. Chem. Thermodyn.* **2006**, *38*, 1396.
- Jacquemin, J.; Husson, P.; Majer, V.; Costa Gomes, M. F. *J. Solution Chem.* **2007**, *36*, 967.
- Baltus, R. E.; Culbertson, B. H.; Dai, S.; Luo, H.; DePaoli, D. W. *J. Phys. Chem. B* **2004**, *108*, 721.

12. Cadena, C.; Anthony, J. L.; Shah, J. K.; Morrow, T. I.; Brennecke, J. F.; Maginn, E. J. *J. Am. Chem. Soc.* **2004**, *126*, 5300.
 13. Kazarian, S. G.; Briscoe, B. J.; Welton, T. *Chem. Commun.* **2000**, *20*, 2047.
 14. Deschamps, J.; Costa Gomes, M. F.; Pádua, A. A. H. *Chem-PhysChem* **2004**, *5*, 1049.
 15. Blanchard, L. A.; Gu, Z.; Brennecke, J. F. *J. Phys. Chem. B* **2001**, *105*, 2437.
 16. Muldoon, M. J.; Aki, S. N. V. K.; Anderson, J. L.; Dixon, J. K.; Brennecke, J. F. *J. Phys. Chem. B* **2007**, *111*, 9001.
 17. Bara, J. E.; Gabriel, C. J.; Lessmann, S.; Carlisle, T. K.; Finotello, A.; Gin, D. L.; Noble, R. D. *Ind. Eng. Chem. Res.* **2007**, *46*, 5380.
 18. Shiflett, M. B.; Kasprzak, D. J.; Junk, C. P.; Yokozeki, A. *J. Chem. Thermodyn.* **2008**, *40*, 25.
 19. Zhang, J.; Zhang, S.; Dong, K.; Zhang, Y.; Shen, Y.; Lv, X. *Chem. Eur. J.* **2006**, *12*, 4021.
 20. Swatloski, R. P.; Holbrey, J. D.; Rogers, R. D. *Green Chem.* **2003**, *5*, 361.
 21. Burrell, A. K.; Del Sesto, R. E.; Baker, S. N.; McCleskey, T. M.; Baker, G. A. *Green Chem.* **2007**, *9*, 449.
 22. Seddon, K. R.; Stark, A.; Torres, M. J. *Pure Appl. Chem.* **2000**, *72*, 2275.
 23. Kuhlmann, E.; Himmeler, S.; Giebelhaus, H.; Wasserscheid, P. *Green Chem.* **2007**, *9*, 233.
 24. Gaină, I.; Bala, D. *Analele Universității București-Chimie XIV* **2005**, 279.
 25. Sinor, J. E.; Schindler, D. L.; Kurata, F. *AIChE Journal* **1966**, *12*, 353.
 26. Bradaric, C. J.; Downard, A.; Kennedy, C.; Robertson, A. J.; Zhou, Y. *Green Chem.* **2003**, *5*, 143.
 27. Camper, D.; Scovazzo, P.; Koval, C.; Noble, R. *Ind. Eng. Chem. Res.* **2004**, *43*, 3049.
 28. Dymond, J. H.; Marsh, K. N.; Wilhoit, R. C.; Wong, K. C. *The Virial Coefficients of Pure Gases and Mixtures*; Springer-Verlag Berlin Heidelberg: 2002; pp 28-30.
 29. Span, R.; Wagner, W. *J. Phys. Chem. Ref. Data* **1996**, *25*, 1509.
 30. Dzyuba, S. V.; Bartsch, R. A. *ChemPhysChem* **2002**, *3*, 161.
 31. Tokuda, H.; Hayamizu, K.; Ishii, K.; Susan, Md. A. B. H.; Watanabe, M. *J. Phys. Chem. B* **2005**, *109*, 6103.
 32. Krause, D.; Benson, B. B. *J. Solution Chem.* **1989**, *18*, 823.
 33. Chen, Y.; Zhang, S.; Yuan, X.; Zhang, Y.; Zhang, X.; Dai, W.; Mori, R. *Thermochim. Acta* **2006**, *441*, 42.
 34. Aki, S. N. V. K.; Mellein, B. R.; Saurer, E. M.; Brennecke, J. F. *J. Phys. Chem. B* **2004**, *108*, 20355.
 35. Jacquemin, J.; Husson, P.; Majer, V.; Pádua, A. A. H.; Costa Gomes, M. F. *Green Chem.* **2008**, *10*, 944.
-